Combined effect of molten fluoride salt and irradiation on Ni-based alloys

A.S.Bakai,

Kharkiv Institute of Physics &Technology, Ukraine
e-mail: bakai@kipt.kharkov.ua

Molten Salt Reactor

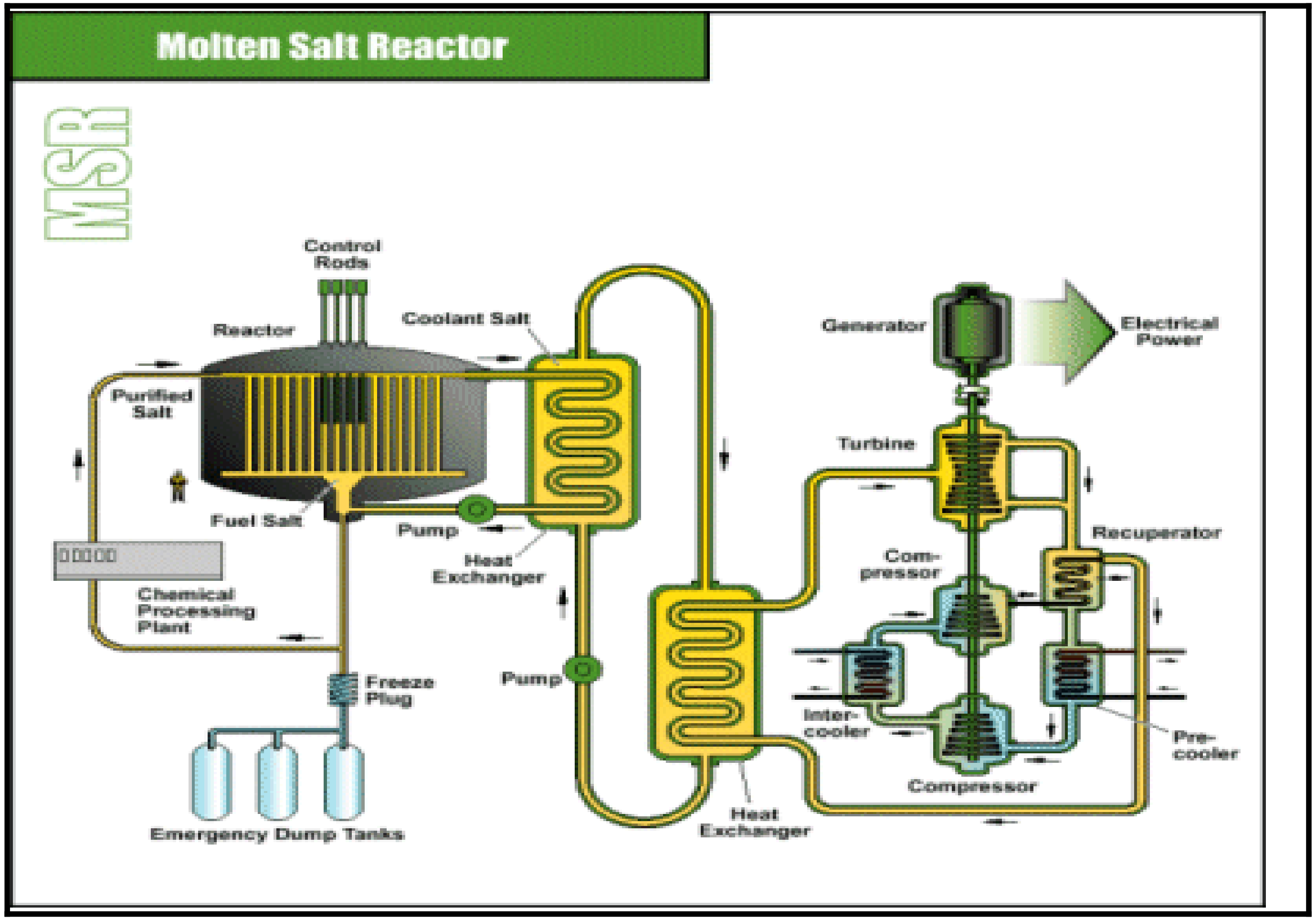

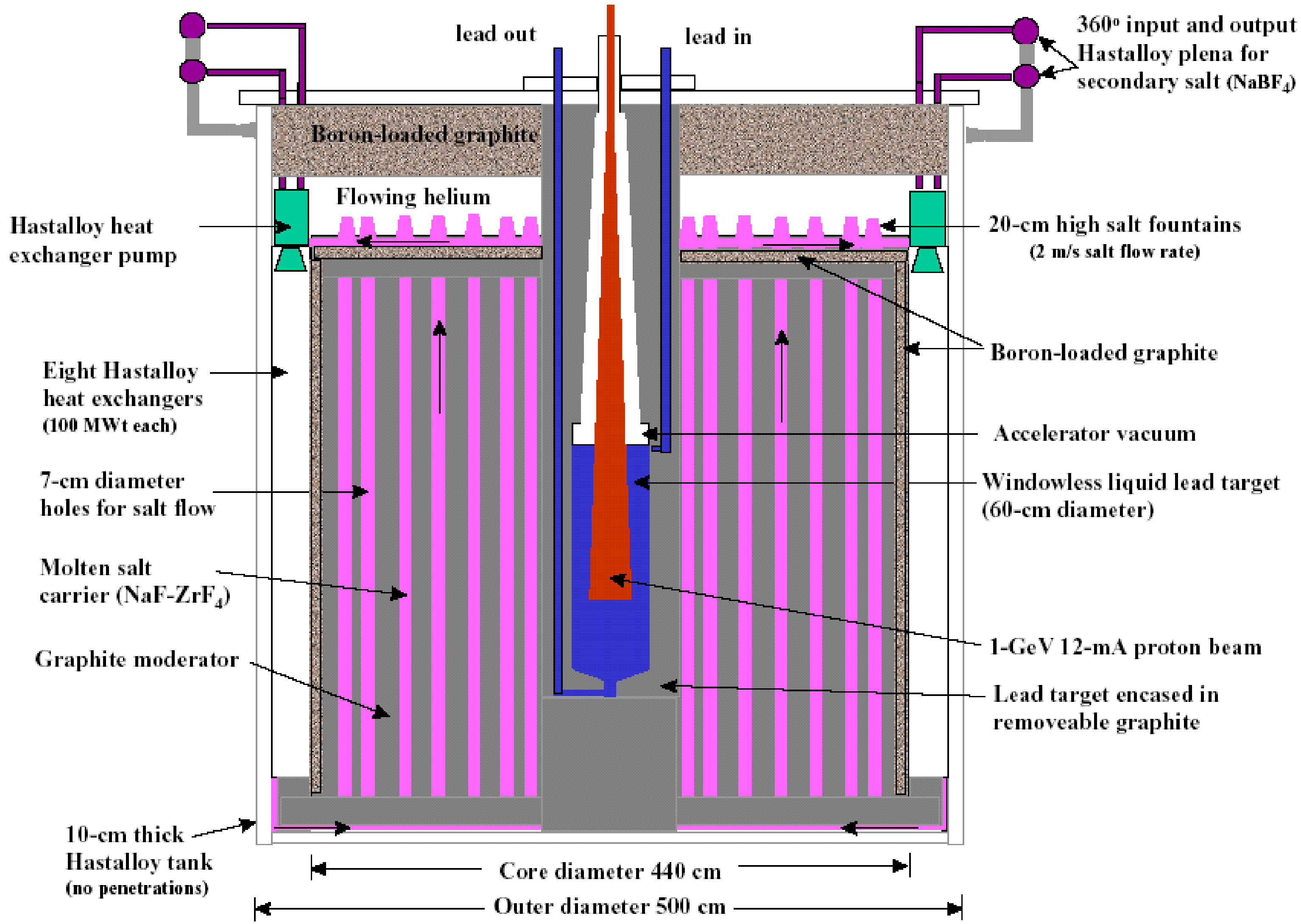

lead out
lead in
360° input and output
Hastalloy plena for
secondary salt ($NaBF_4$)
Boron-loaded graphite
Flowing helium
Hastalloy heat
exchanger pump
20-cm high salt fountains
(2 m/s salt flow rate)
Boron-loaded graphite
Eight Hastalloy
heat exchangers
(100 MWt each)
Accelerator vacuum
7-cm diameter
holes for salt flow
Windowless liquid lead target
(60-cm diameter)
Molten salt
carrier (NaF-ZrF_4)
1-GeV 12-mA proton beam
Graphite moderator
Lead target encased in
removeable graphite
10-cm thick
Hastalloy tank
(no penetrations)
Core diameter 440 cm
Outer diameter 500 cm

Background

- MSR's and accelerator-driven transmutation technology now under world-wide investigation.
- Various approaches being studied involve molten salt blanket or coolant.
- Corrosion and structural integrity of structural components under irradiation are issues requiring study.
- In the current project electron irradiation at 10 MeV was chosen to simulate neutron irradiation, since the focus of this experiment is on corrosion, a near-surface phenomenon.
- While neutrons affect bulk properties, corrosion is more impacted by near-surface properties and defects, and by softer parts of the spectra, electrons and gamma radiation.
- Material development is also a strong part of this project, with a strong focus on investigation of dopants (Nb, Y) impact on the corrosion. Impact of irradiation and molten salt on C-C composite was investigated, too.

Methodology

- Electron Irradiation Test Facility (EITF)
- Simulations of the e- and gamma- fields and deposited energy distribution in EITF and MSR
- Temperature distribution
- Mechanical tests
- Structure and composition investigations
- Corrosion (voltammetric) tests
- Roentgen Spectroscopy
- Thermodynamics of Zr in alkali halide melts
- Theoretical models

Electron Irradiation Test Facility

- **Irradiation conditions:**
- **Energy:** 10 MeV electrons
- **Temperature:** 650°C / 700 h
- **Current density:** 1.25 □A/cm2
- **Total dose:** 2x10-3 dpa

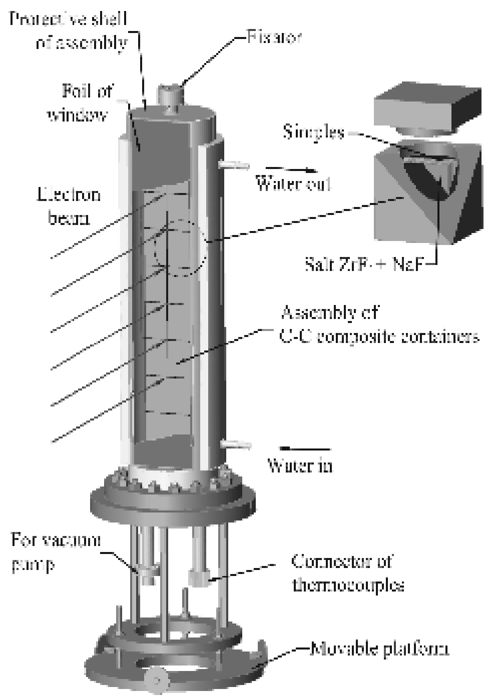

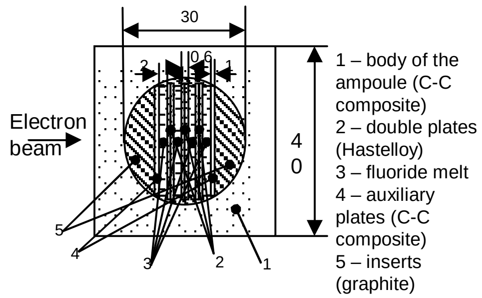

Загальний вигляд опромінювального стенду EITF-KIPT на виході прискорювача ЛПЕ-10

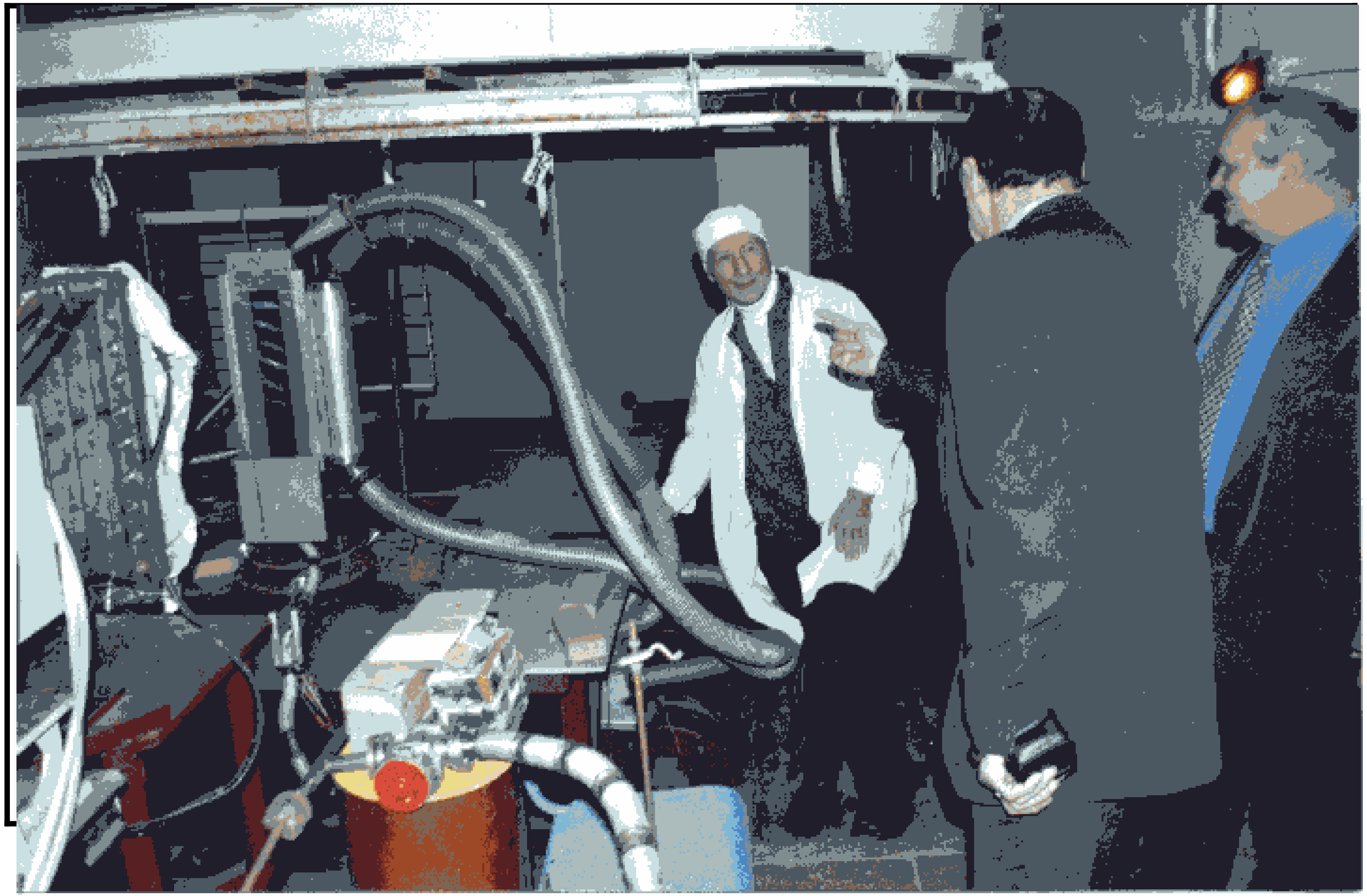

Compositions of Ni-Mo alloys A and B

Element	Alloy A (wt %)	Alloy B (wt %)
Nickel	78.2	78.2
Molybdenum	11.7	11.7
Chromium	6.7	6.2
Titanium	0.5	0.5
Aluminum	0.8	0.8
Iron	1.5	1.5
Manganese	0.5	0.5
Silicon	0.15	0.15
Niobium	-	0.5
Yttrium	-	0.05

In alloy B 0,5 wt% of Nb and 0.05 wt% of Y are alloyed

Ni-Mo phase diagram

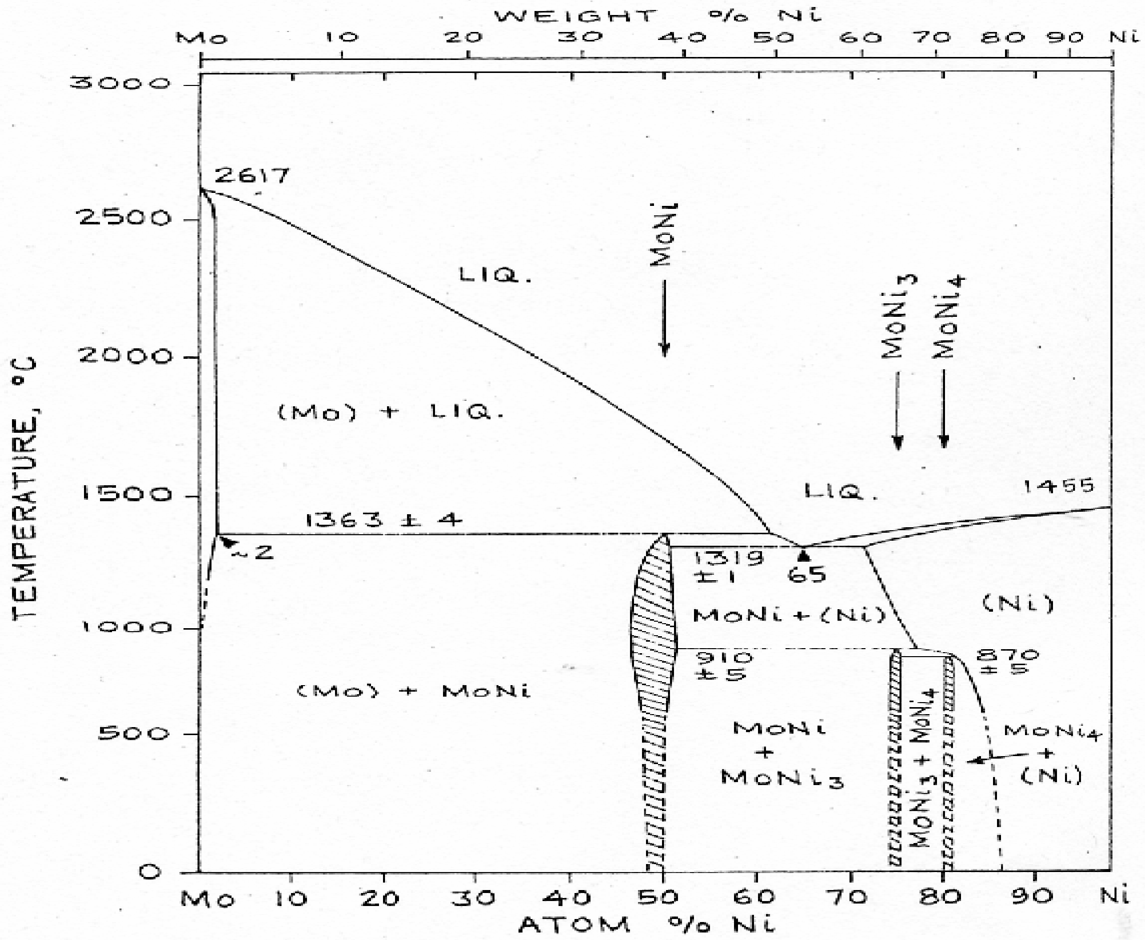

Diagram redrawn from ref. 1 which reviews the literature through 1978. It is essentially the same as that of Shunk Fig. 162; the ref. contains equations for several phase boundaries.

(1) Brewer, L. and Lamoreaux, R.H. P. 289 of "II. Phase Diagrams.", in volume ATOMIC ENERGY REV., SPEC. ISSUE No. 7 ("Molybdenum: Physico-Chemical Properties of its Compounds and Alloys."); L. Brewer, Editor; Internat. Atomic Energy Agency, Vienna; 1980.

Depths dependencies of the deposited power (black circles) and the Ni–Mo alloy A dpa rate (open circles)

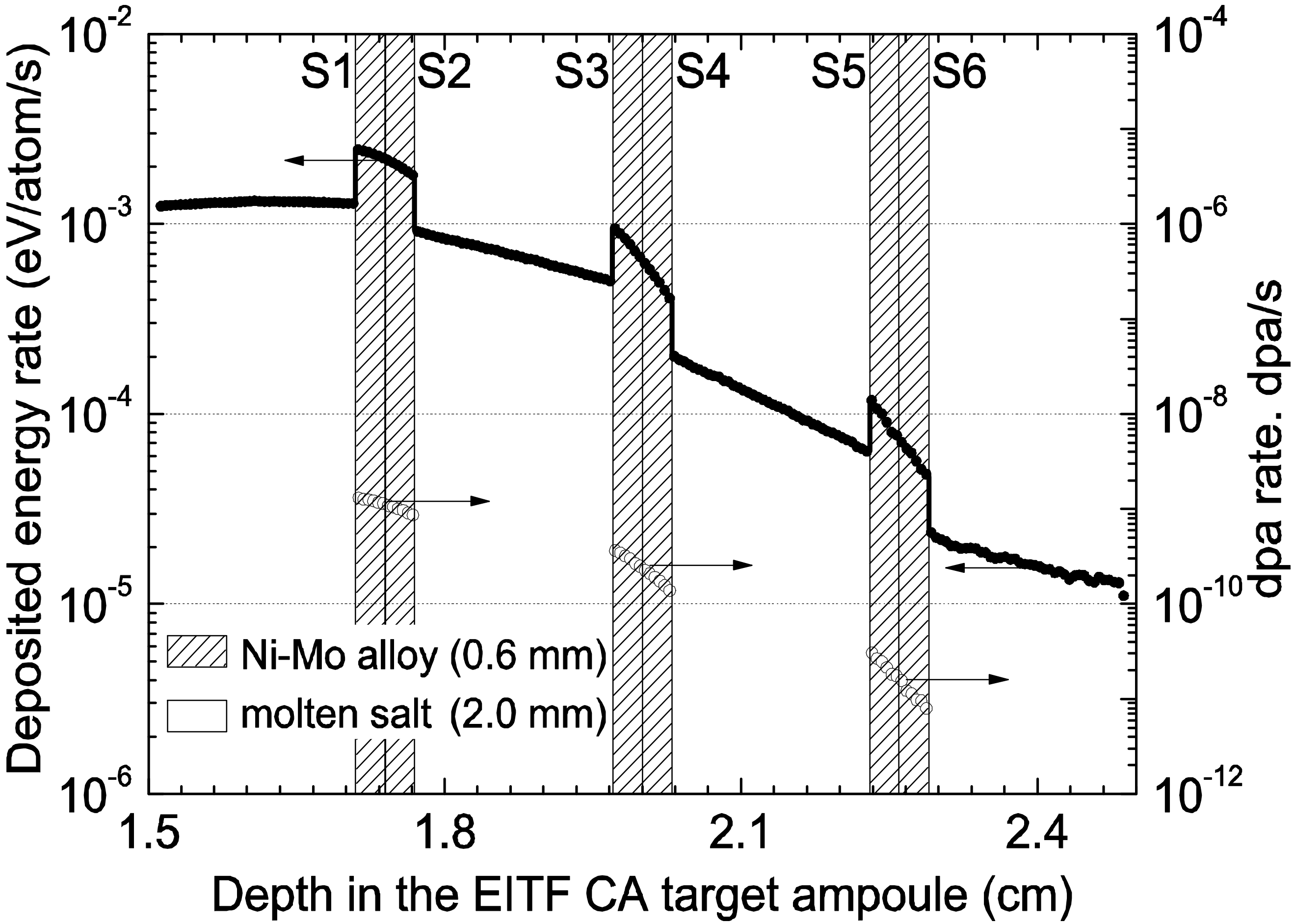

Metallography, etched specimens

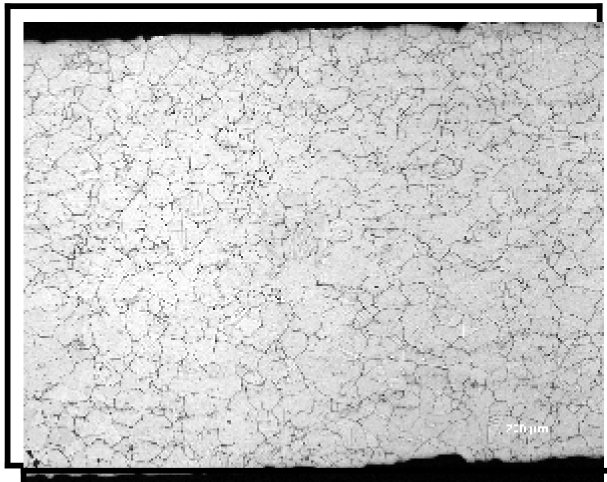

A -0, unirradiated

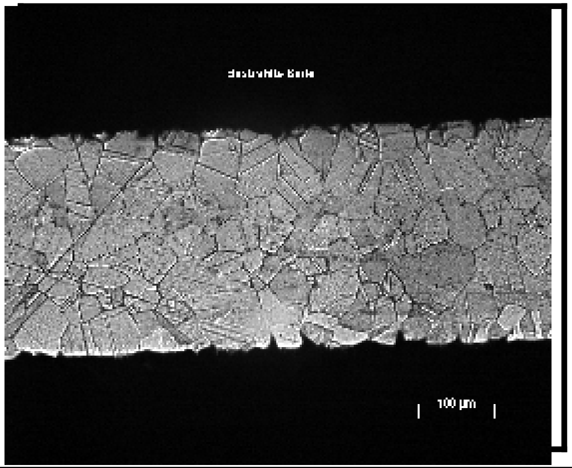

A-1, irradiated

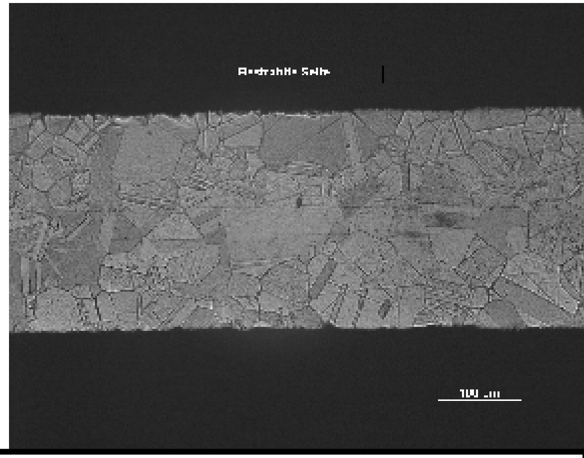

A-6, irradiated

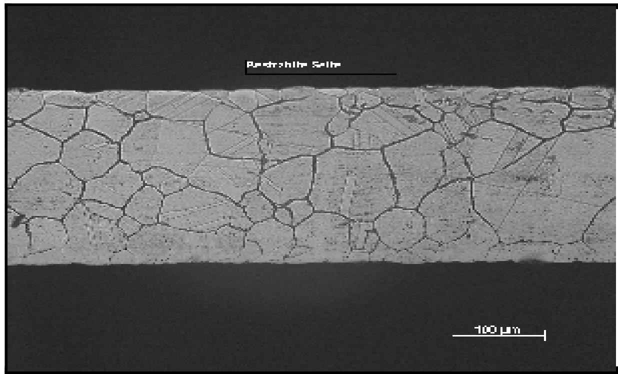

B-2, irradiated

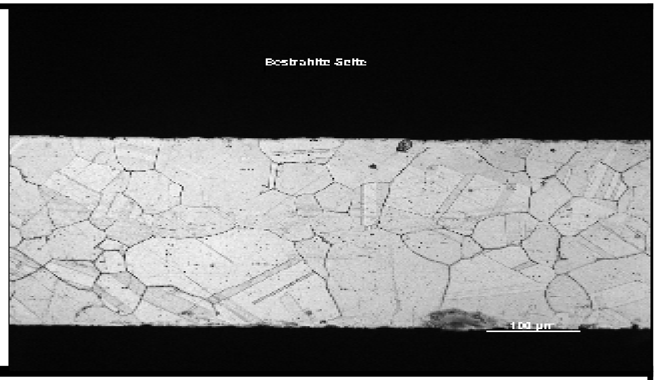

B-5, irradiated

REM and REMMA, Hasrelloy A, unirradiated

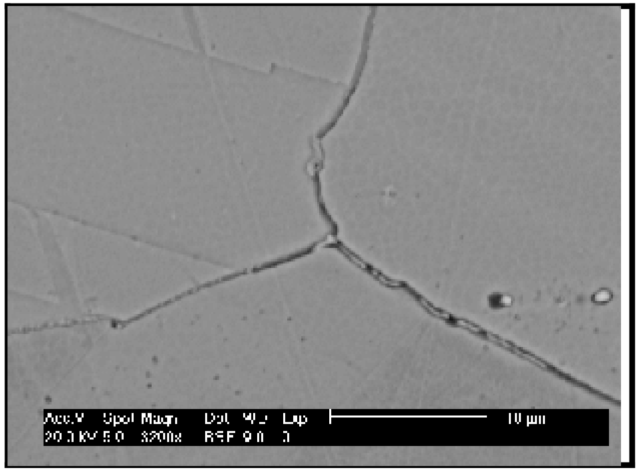

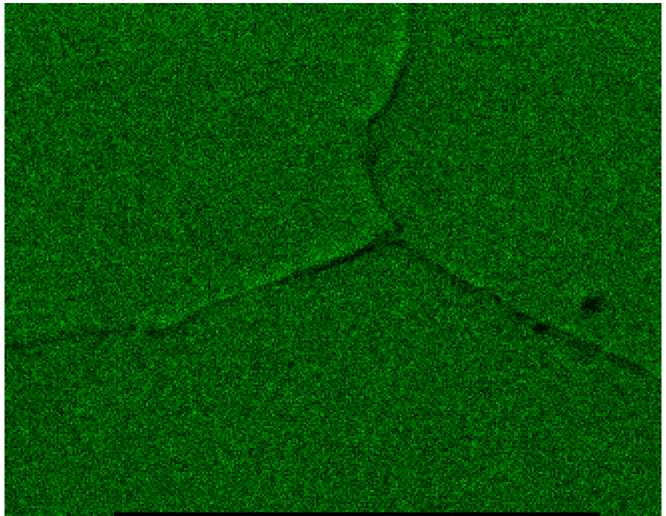

Ni, A-0

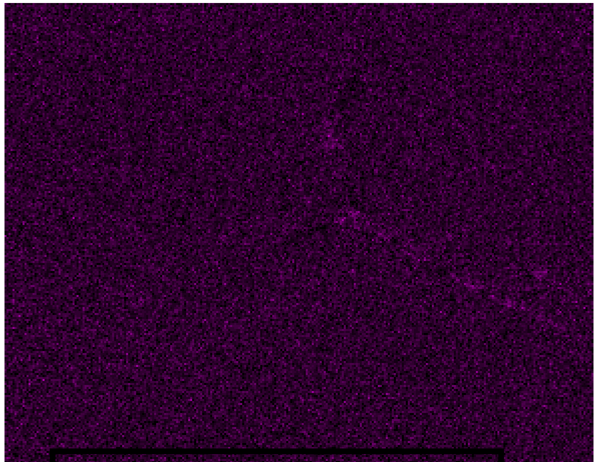

Ti, A-0

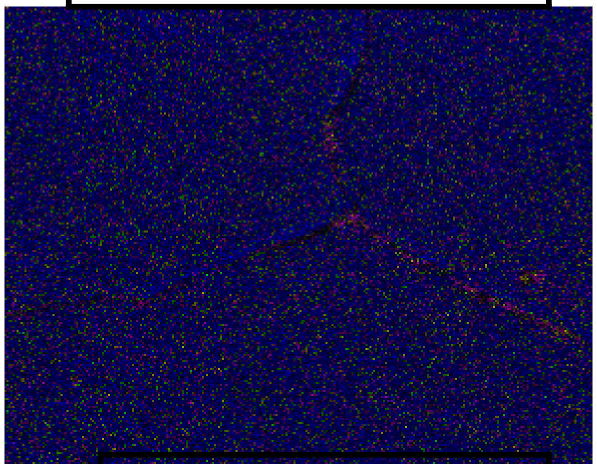

Overlay, A-0

Alloy B before irradiation
(L12 precipitetes composition)

o

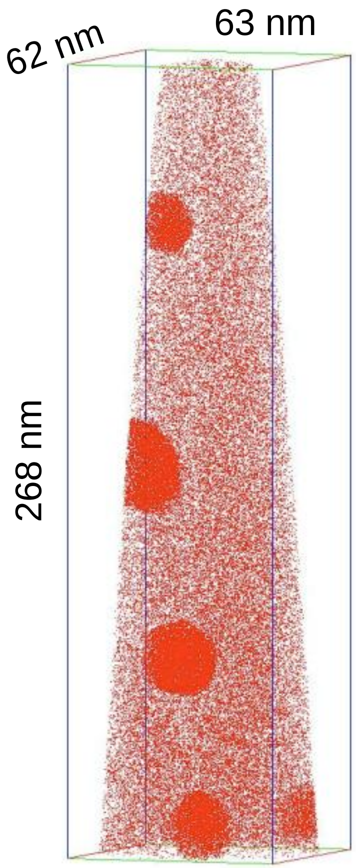

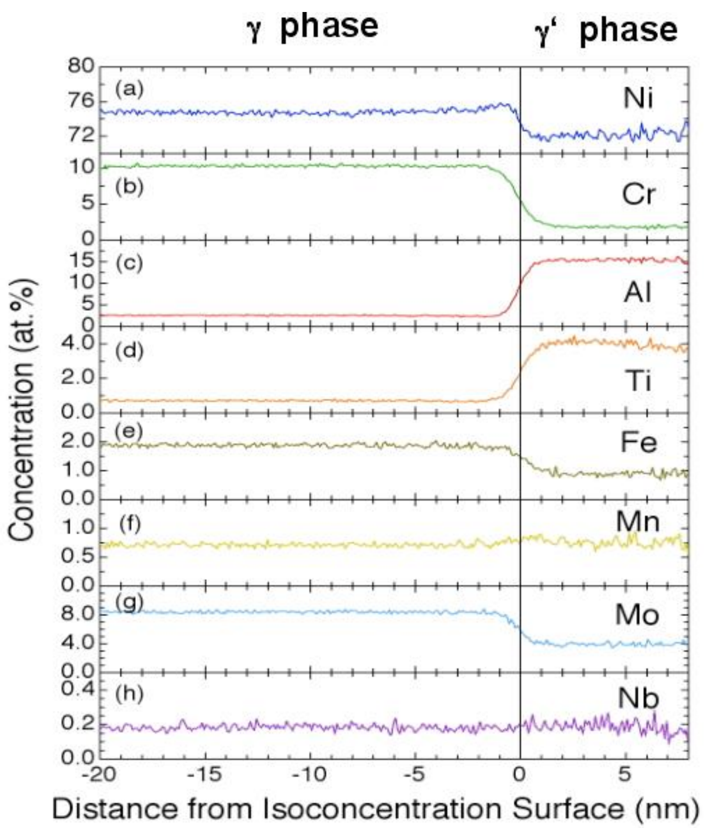

Alloy B, unirradiated, (phase nano-structure)

Al atoms are shown in red color. Precipitates of $L1_2$ structure are seen

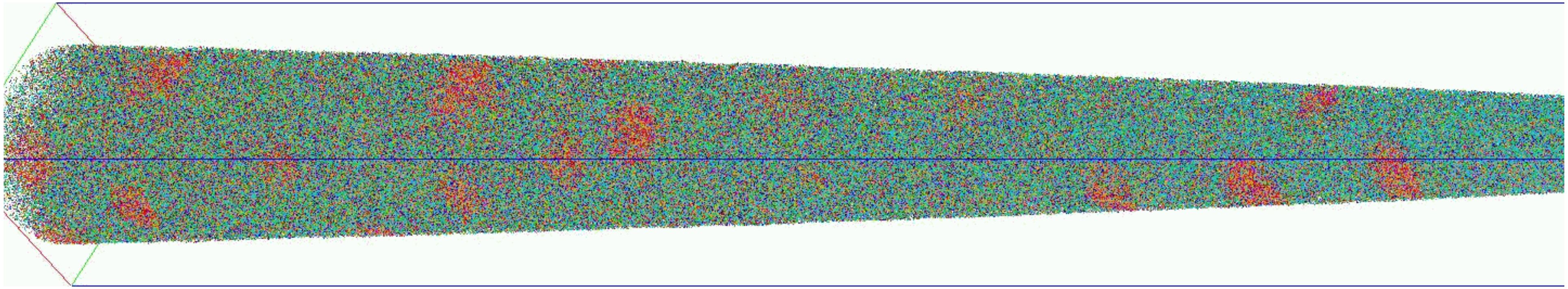

N. Wanderka, D. Isheim (2007)

Irradiated in molten salt Alloy A: macrostructure

- a

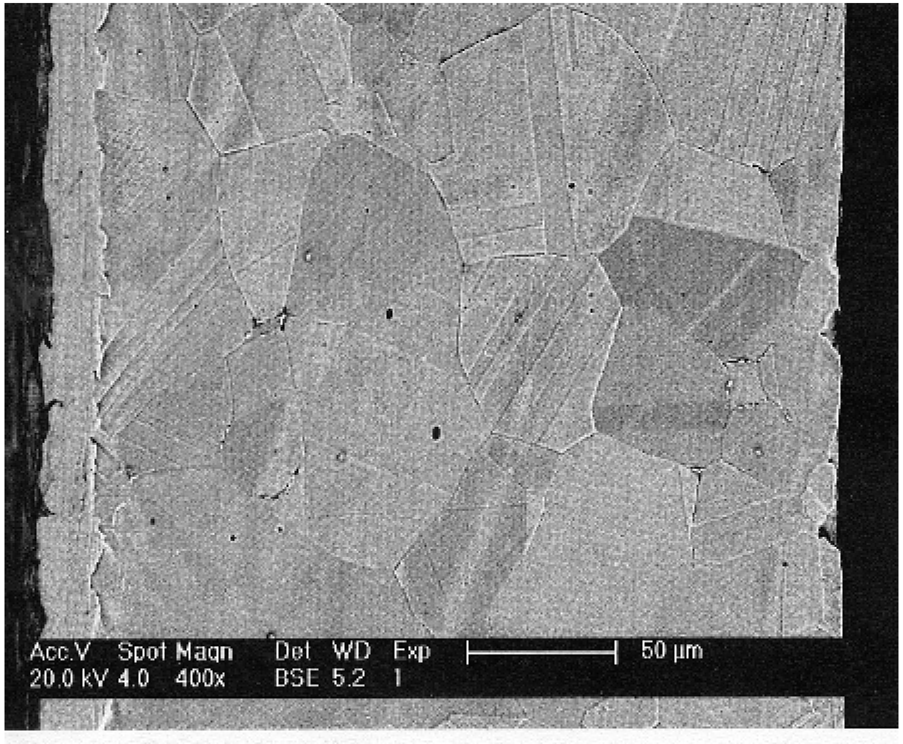

Low precipitation. Macroscopic precipitates in grains and grain boundaries are seen

Alloy B after irradiation (macrostructure)

SEM image of the irradiated Hastelloy

Grain boundaries are decorated by large precipitates

No changes in the composition were measured

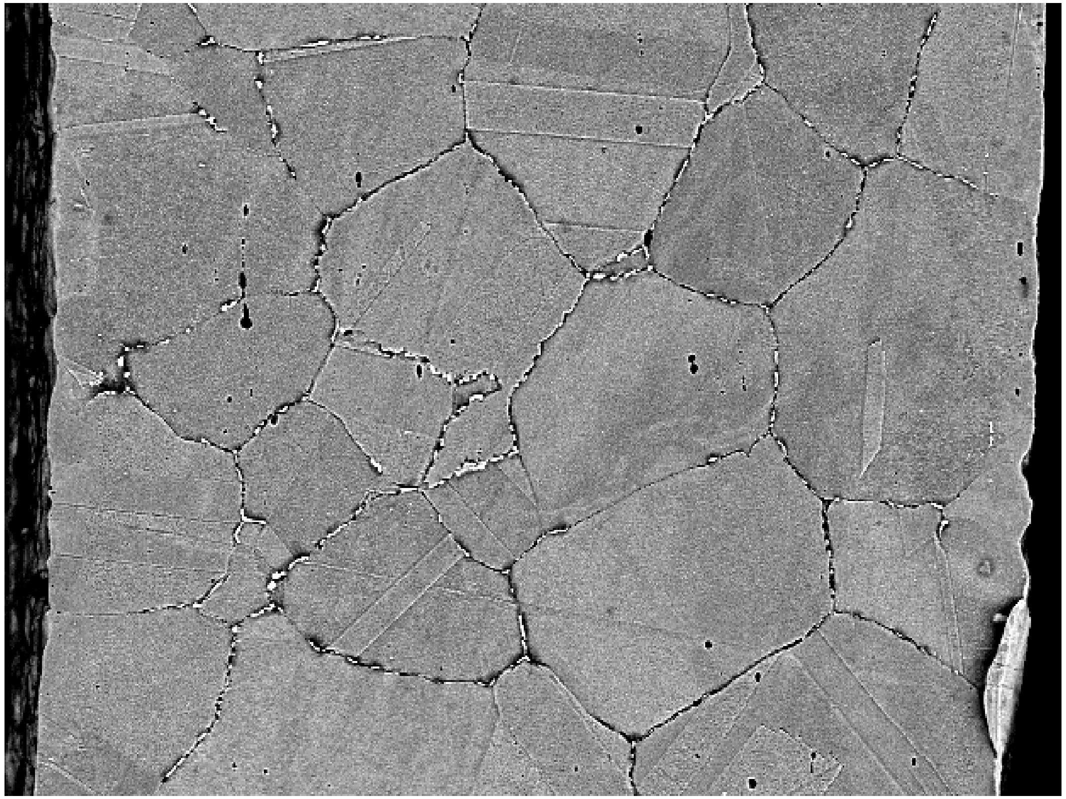

3DAP Analysis: <u>Alloy B, initial state</u>

Ni - 7.3 Mo -7.2Cr - 1.6 Fe - 1.8 Al - 0.6 Ti - 0.5 Mn - 0.3 Nb - 0.3 Si - 0.03 Y (at.%)

Mo-rich Clusters

3D reconstruction of Mo and Ni

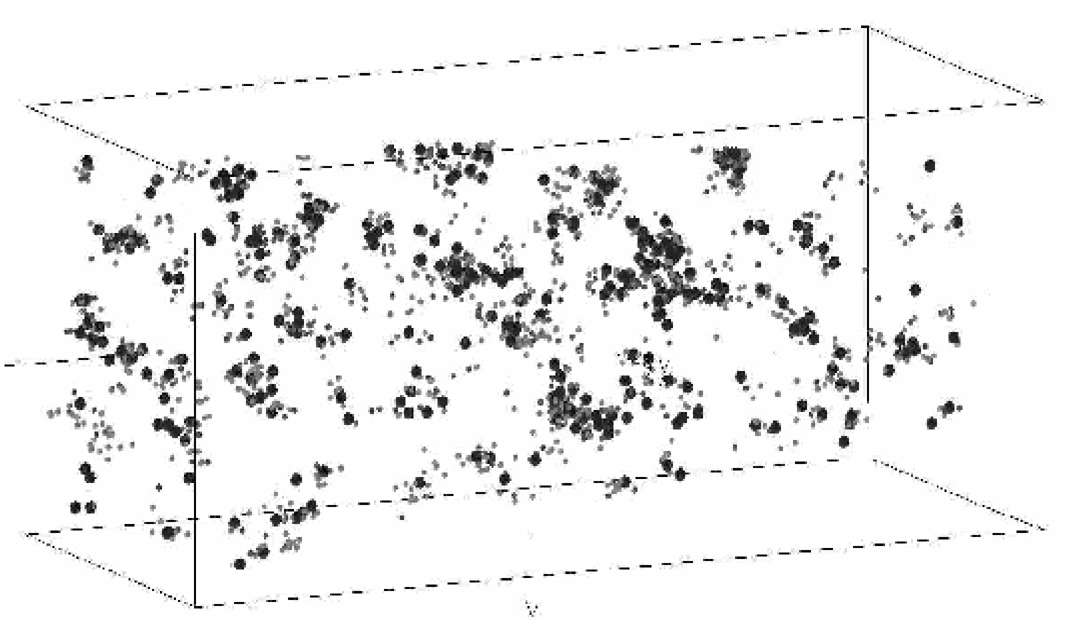

Analyzed volume: 15 x 15 x 24 nm3

Composition (at.%)

Al	2.37
Ni	**67.18**
Cr	8.4
Ti	0.72
Fe	2.54
Mo	**17.6**
Mn	0.88

80 **Ni** – 20**Mo**

Ø clusters 1-3 nm

The Mo-enriched clusters of Ni_4Mo SRO of 2-4 nm in size are seen

Alloy B: initial state (microstructure)

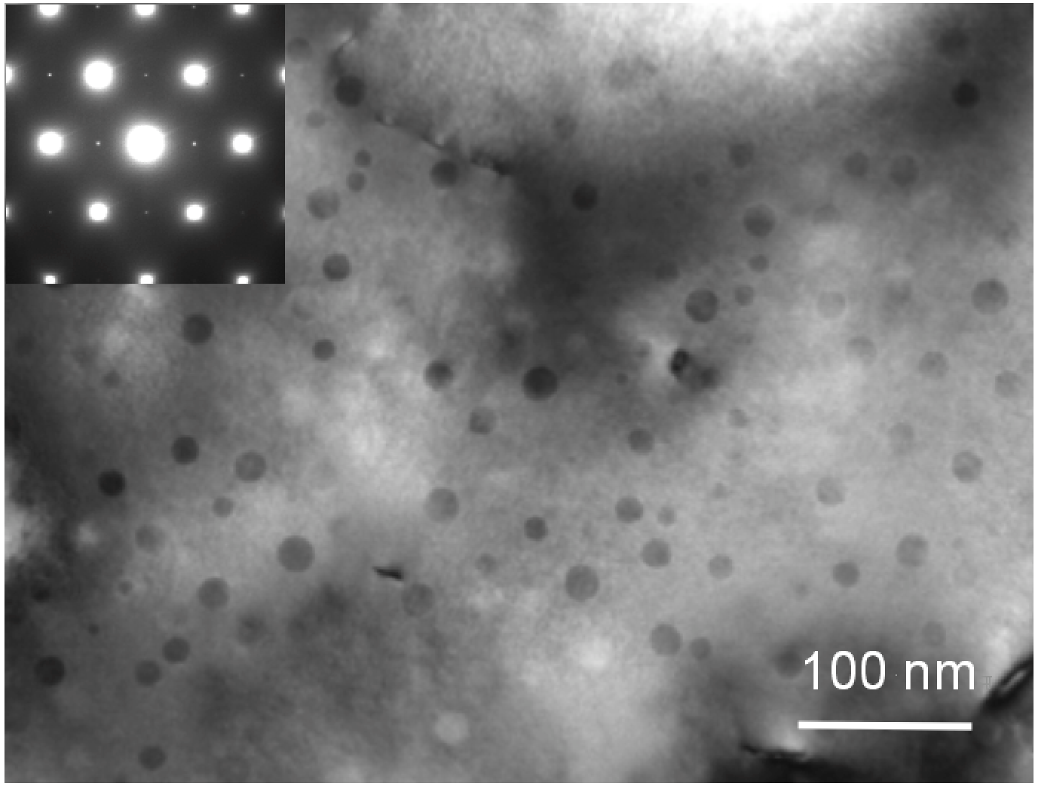

Homogeneously distributed small spherical precipitates with L12-type ordering have been formed in the interior of the grains. The [011] zone-axis electron-diffraction pattern (inset) exibits L12–type superlattice reflections.

BF TEM image and corresponding SAD pattern in <100> direction of matrix of irradiated alloy B. Small precipitates, Ǿ~10nm, are formed. The supper reflexes arising from the precipitates are of D022 (Ni_4Mo) short range order

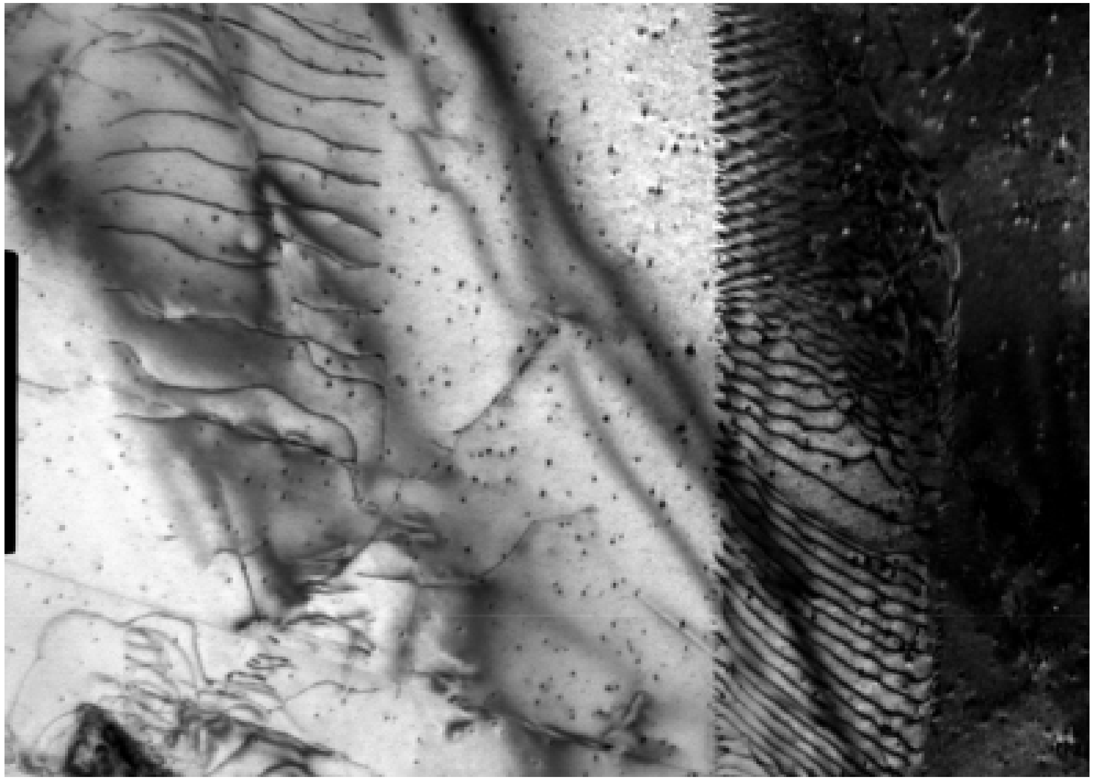

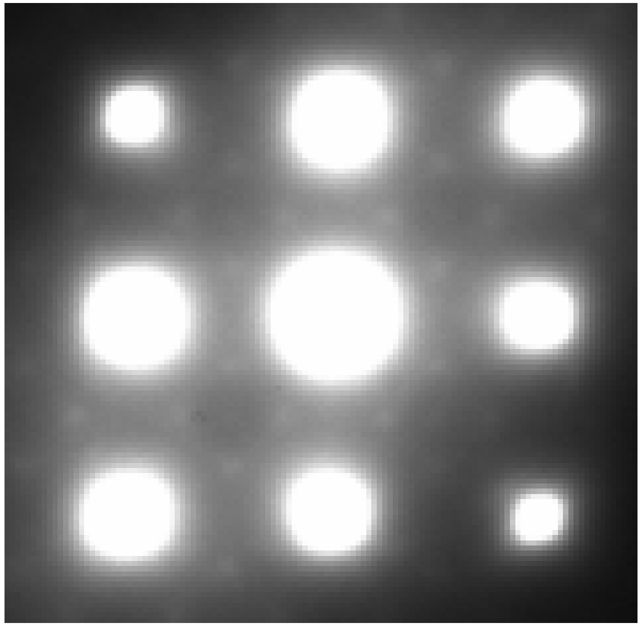

TEM Analysis: Alloy B after e- irradiation (first plate, 5066 ev/at)

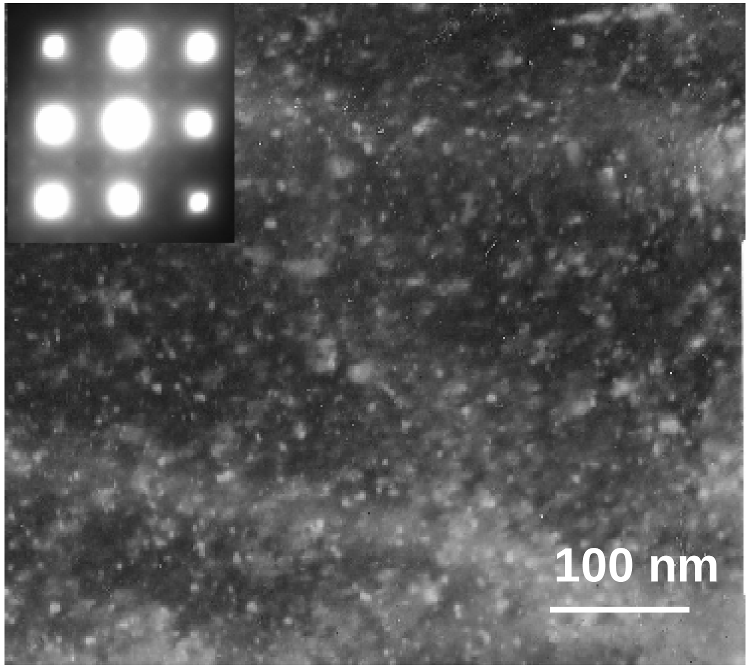

DF TEM

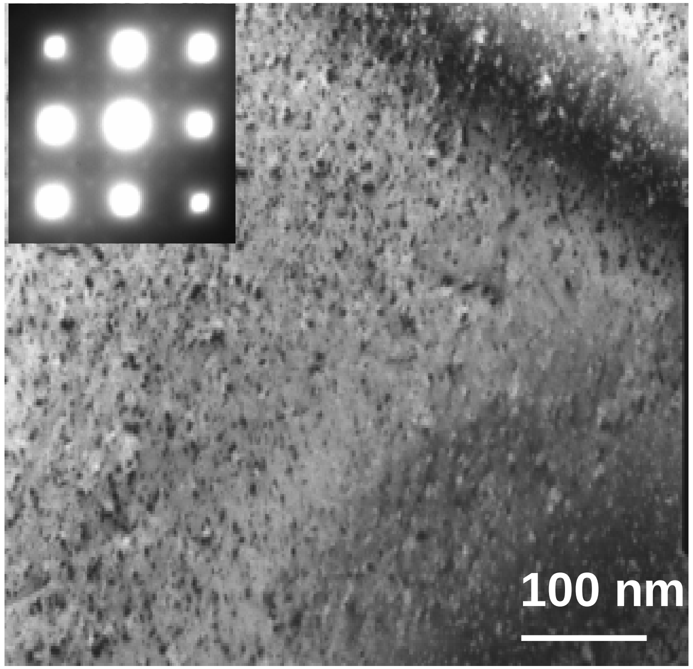

BF TEM

No spherical precipitates and no $L1_2$ supper reflections are visible,
Only small precipitates with SRO are visible

TEM Analysis: Alloy B after e- irradiation (second plate)

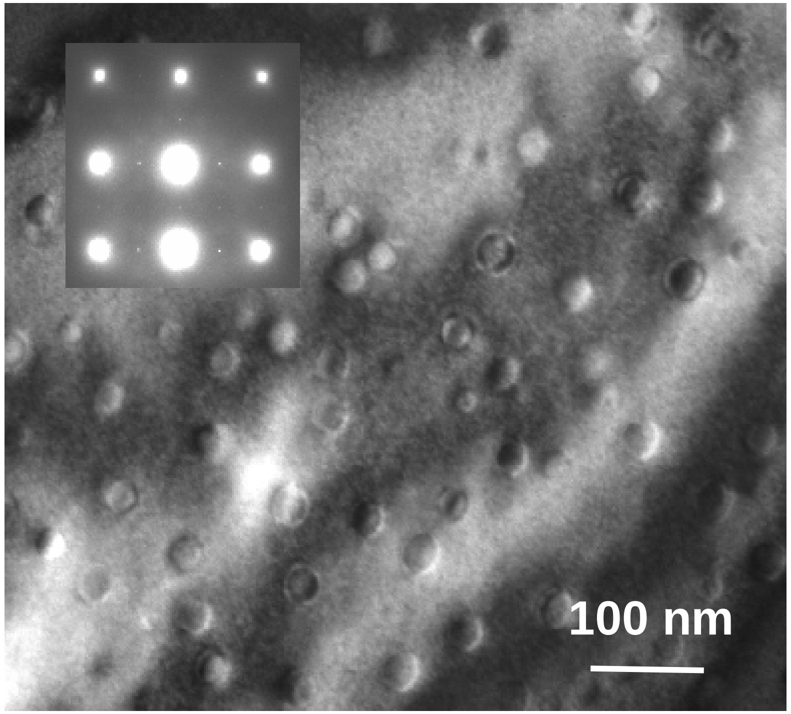

DF TEM

Spherical precipitates are visible

weak supper reflections of $L1_2$ and SRO

TEM/ SAD Analysis: AlloyB before and after e-irradiation

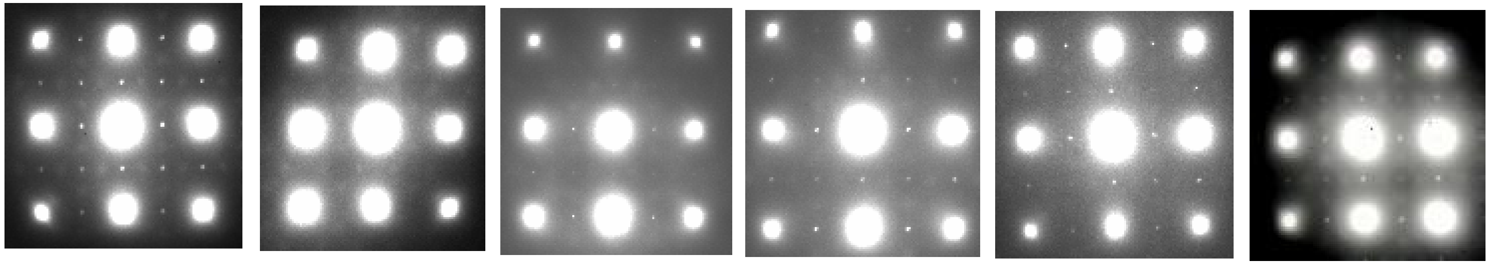

B0 B131 B132 B13 3 B134 B139

Mechanical properties of alloys A and B

Material	Test temperature, °C	E_{dep}, eV/atom	σ_B, MPa	σ_{02}, MPa	δ, %
Hastelloy-A, Initial structure, aged for 50 hours at 675°C	20	0	900	395	63
	600	0	397	288	14
Hastelloy-A, 700 hours in salt at 650°C	20	0	1070	875	43
		120	848	576	54
		6190	626	333	35
	650	0	510	440	9
		120	362	255	15
		6190	276	213	15
Hastelloy-B, Initial structure, aged for 50 hours at 675°C	20	0	845	397	53
	600	0	443	310	19
Hastelloy-B, 700 hours in salt at 650°C	20	120	851	415	48
		6190	876	333	50
	650	120	350	318	15
		6190	293	214	15

Along with high plasticity the irradiated specimens are considerably softer (see σ_{02} values) than those without irradiation

Corrosion rates of Alloys A and B at 650°C in molten fluoride salt with and without irradiation

- Irradiation increases the corrosion rates in molten fluoride salt by 100 – 1000 times
- Corrosion rate of the alloy B is proportional to the deposited energy

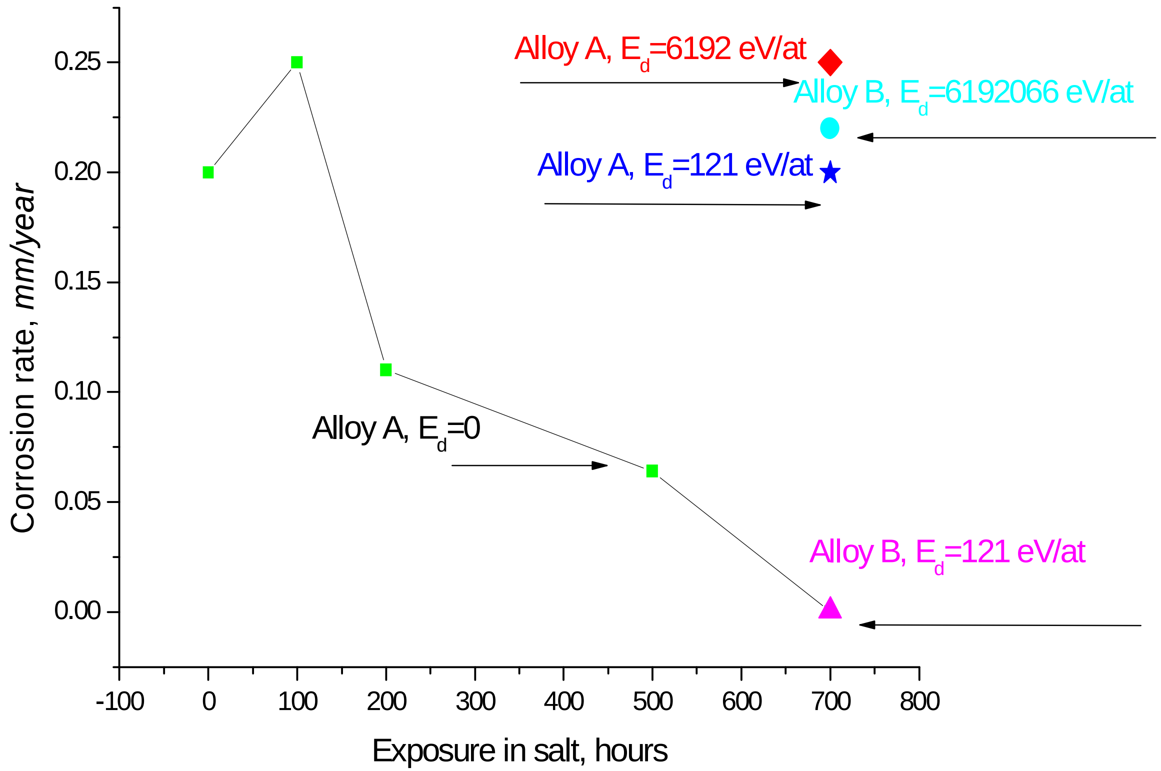

Compositional changes in surface layers of Hastelloy A

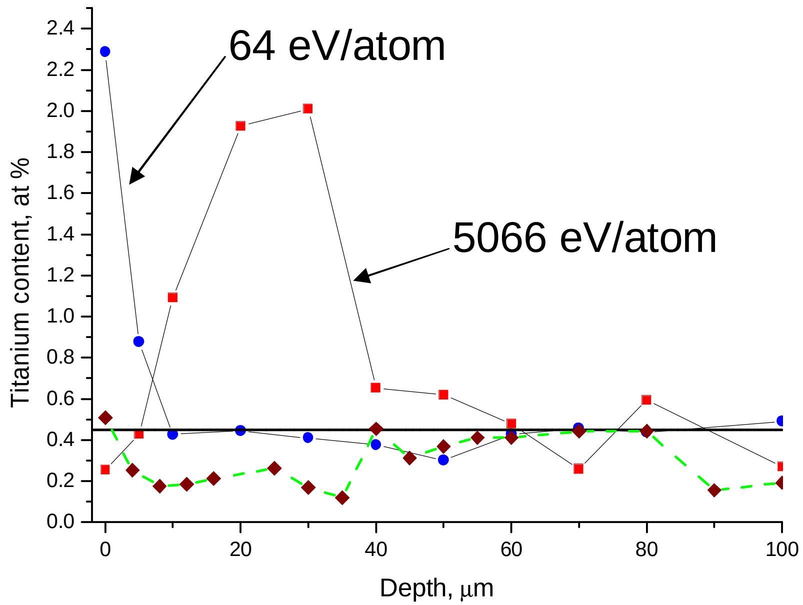

Redistribution of the Ti content after 700 hours exposure in molten salt without and under e-irradiation at 650°C

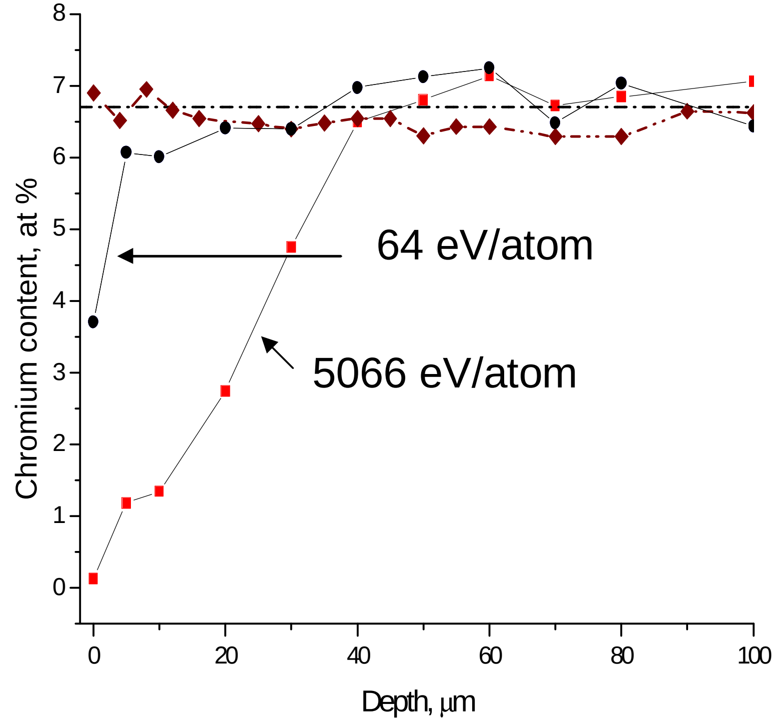

Redistribution of the Cr content after 700 hours exposure in molten salt without and under e-irradiation at 650°C

eV/atom is the total deposited energy in surface layer

Loading and unloading curves during nano-indentation of C-C composite before and after irradiation in molten salt at 600°C

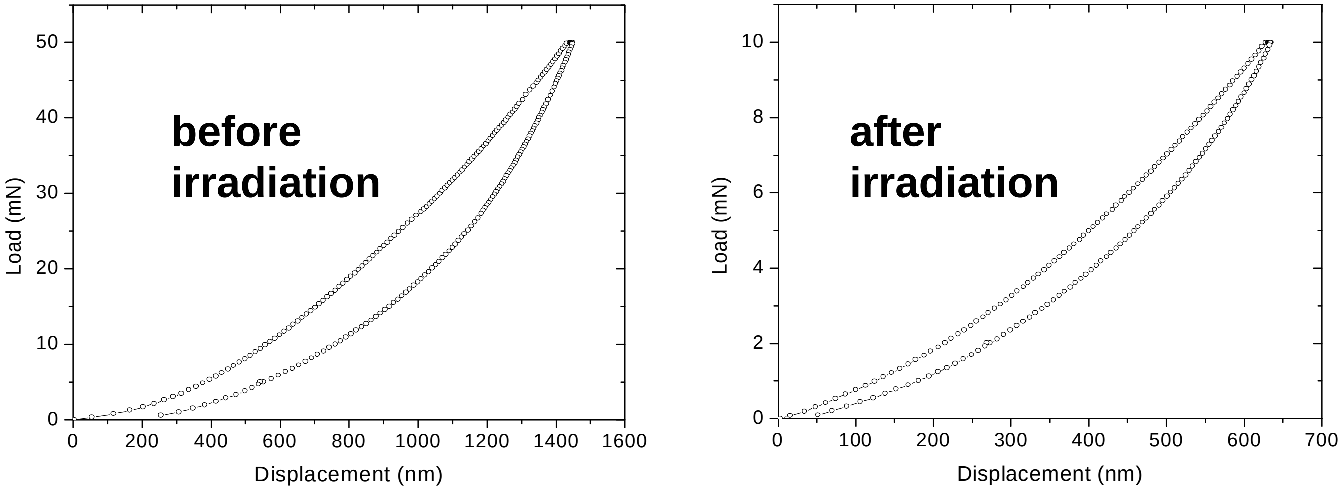

Hardness and elastic modulus were to be determined from the depth of indentation according to the Oliver and Farr technique.

Microscopic examination did not reveal indentations on the samples as this material has a high capacity for the elastic recovery of the original shape.

Material appears to be a form of "glassy carbon", which is amorphous carbon with sp^2 bonds predominating.

Depths dependencies of the deposited power (black circles) and the Ni–Mo alloy A dpa rate (open circles)

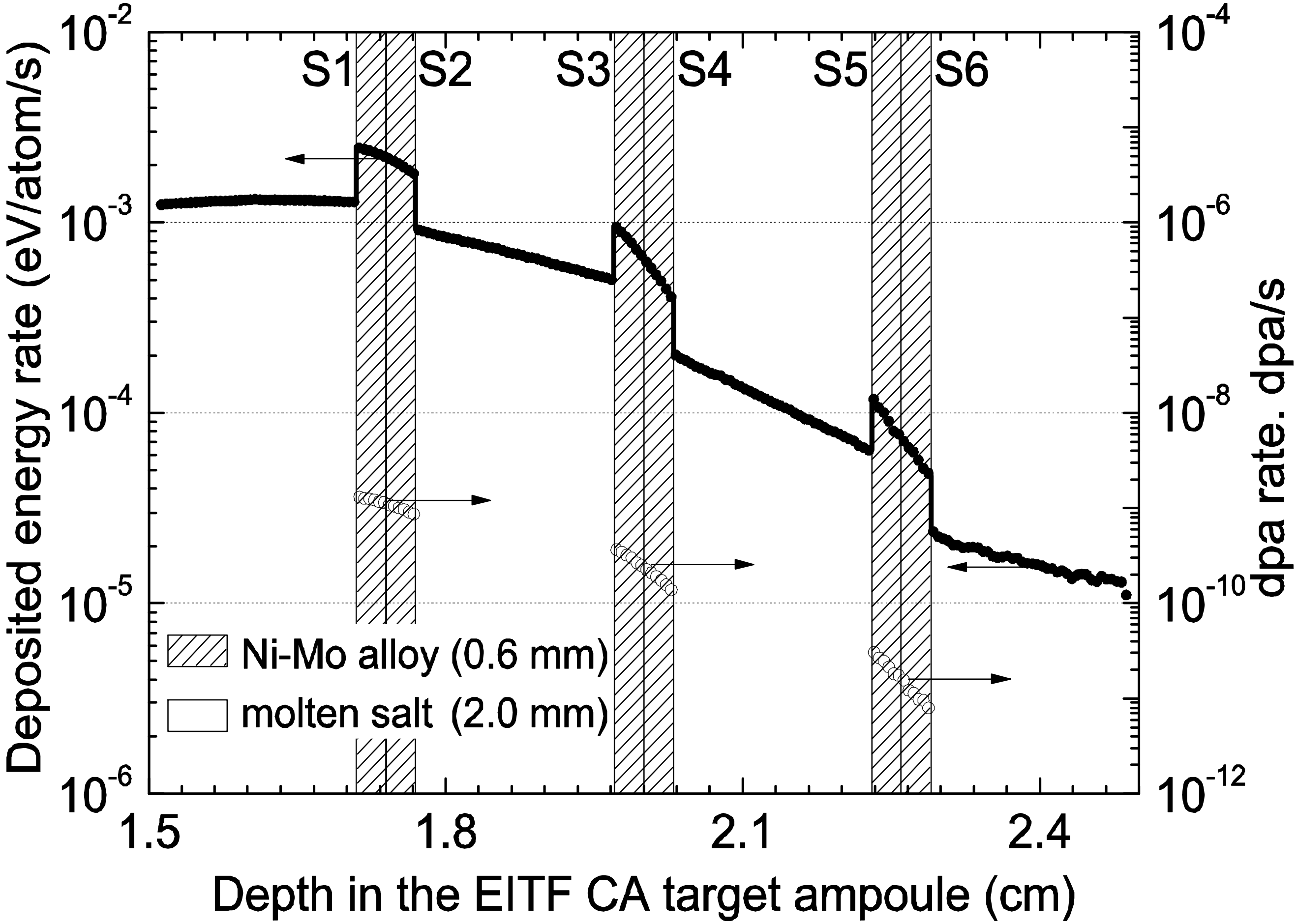

Energy-weighted neutron (a) and photon (b) spectra of MSR cores with different moderator-to-fuel (C/MS) ratios. (the total neutron flux f_0 = 10^15 cm^-2·s^-1)

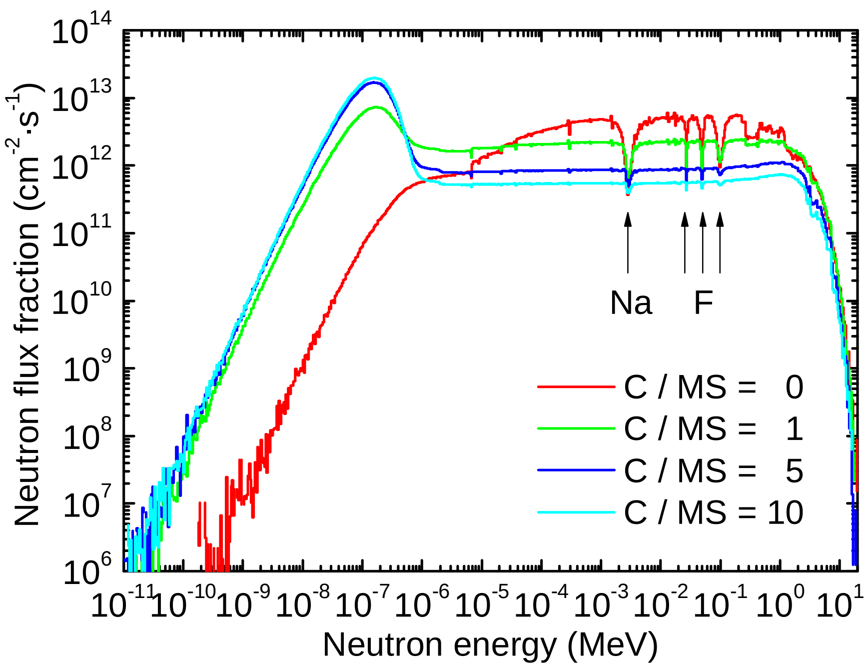

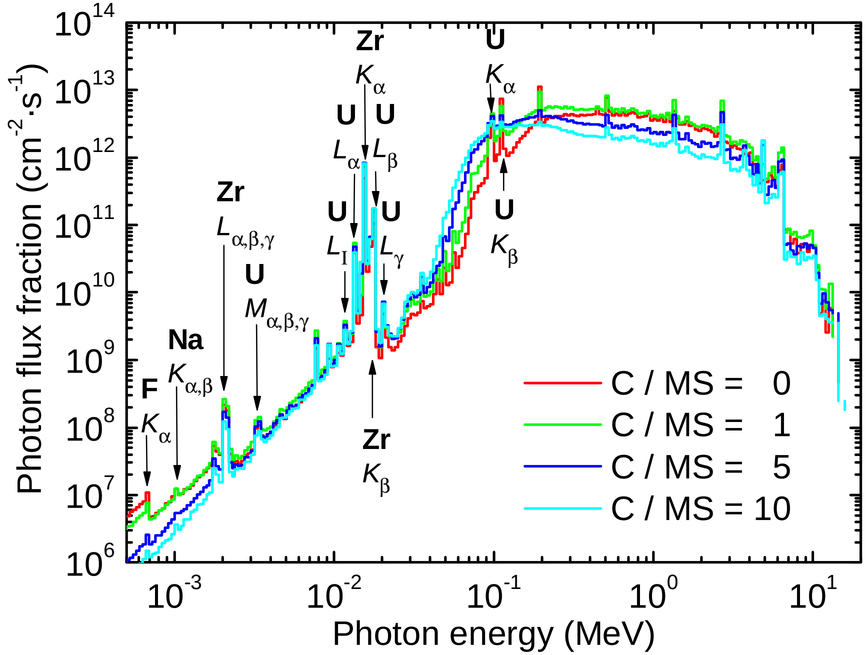

- **(a) neutron spectra**
- **(b) photon spectra**

A. S. Bakai, M. I. Bratchenko and S.V. Dyuldya, 2007

Deposited Energy
and Radiation damage in EITF and MSR’s

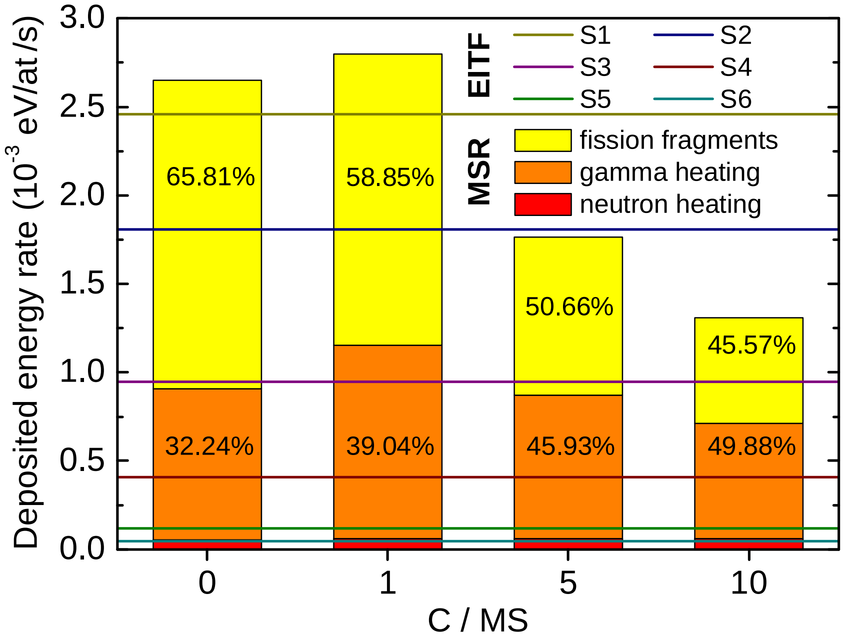

(a) Deposited Energy

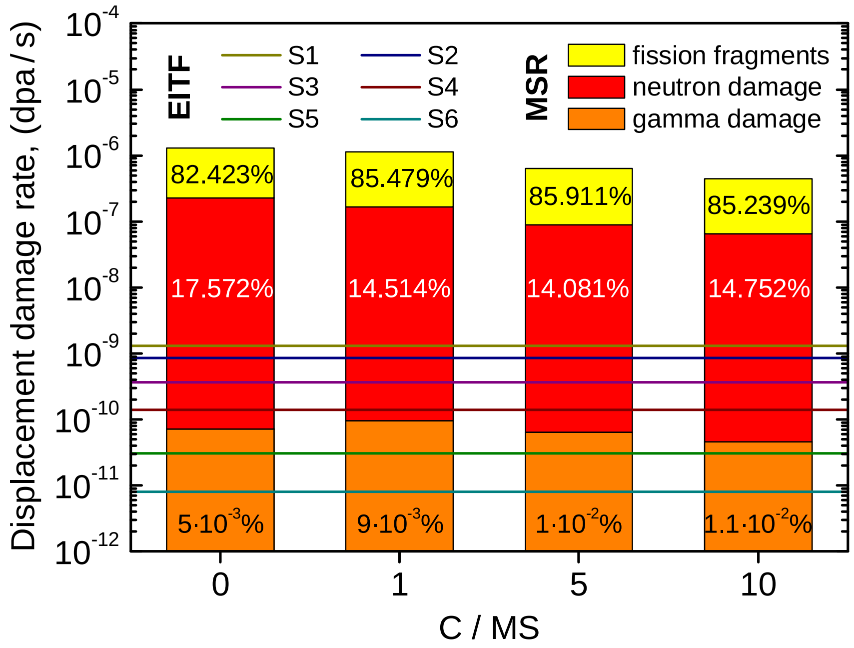

(b) Radiation damage
(Frenkel’s pair generation)

Conclusions

- EITF is an efficient device for corrosion tests of G-IV candidate construction materials.
- EITF electron beam irradiation is capable to reproduce realistic irradiation conditions of G-IV molten salts reactor concerning the major factor affecting the Ni–Mo alloys corrosion, the energy deposition in surface layers of alloys.
- Ni–Mo alloys A and B have acceptable corrosion resistance in molten fluoride salt at 650°C. After electron irradiation in EITF for 700 h the voltammetric data provide estimation of the corrosion rate to be ~0.1 mm/year.
- The corrosion mode and resistance is rather sensitive to Nb and Y and presumably to other dopants. The alloy doped with Nb (0.5%) and Y (0.05%) does not show considerable intercrystalline corrosion, but its corrosion rate is sensitive to the deposited energy dose.

Conclusions 2

- Optimization of the composition has to be made to minimize the corrosion rate.
- Precipitates, located mainly in grain boundaries, contain a lot of Y and apparently they work as getters mitigating the intercrystalline corrosion attack.
- Structure, composition and SRO of nano-scale precipitates in Ni–Mo alloys is evolving under irradiation. This fact has to be taken into account at R&D of advanced materials for G-IV reactors.